Atmos. Chem. Phys. Discuss., 13, 10157–10192, 2013
www.atmos-chem-phys-discuss.net/13/10157/2013/
doi:10.5194/acpd-13-10157-2013

Atmospheric Chemistry and Physics Discussions
Open Access

Airborne observations and modeling of springtime stratosphere-to-troposphere transport over California

E. L. Yates[1], L. T. Iraci[1], M. C. Roby[2], R. B. Pierce[3], M. S. Johnson[1], P. J. Reddy[4], J. M. Tadić[1], M. Loewenstein[1], and W. Gore[1]

[1]Earth Sciences Branch, NASA Ames Research Center, Moffett Field, CA 94035, USA
[2]Department of Meteorology, San Jose State University, San Jose, CA 95192-0104, USA
[3]NOAA/NESDIS Advanced Satellite Products Branch Madison, WI 53706, USA
[4]Air Pollution Control Division, Colorado Department of Public Health & Environment, Denver, CO 80246, USA

Received: 6 March 2013 – Accepted: 2 April 2013 – Published: 18 April 2013

Correspondence to: E. L. Yates (emma.l.yates@nasa.gov)

Published by Copernicus Publications on behalf of the European Geosciences Union.

Abstract

Stratosphere-to-troposphere transport (STT) results in air masses of stratospheric origin intruding into the free troposphere. Once in the free troposphere, O_3-rich stratospheric air can be transported and mixed with tropospheric air masses, contributing to the tropospheric O_3 budget. Evidence of STT can be identified based on the differences in the trace gas composition of the two regions. Because ozone (O_3) is present in such large quantities in the stratosphere compared to the troposphere, it is frequently used as a tracer for STT events.

This work reports on airborne in situ measurements of O_3 and other trace gases during two STT events observed over California, USA. The first, on 14 May 2012, was associated with a cut-off low, and the second, on 5 June 2012, occurred during a post-trough, building ridge event. In each STT event, airborne measurements identified high O_3 within a stratospheric intrusion which was observed as low as 3 km above sea level. During both events the stratospheric air mass was characterized by elevated O_3 mixing ratios and reduced carbon dioxide (CO_2) and water vapor. The reproducible observation of reduced CO_2 within the stratospheric air mass supports the use of non-conventional tracers as an additional method for detecting STT. A detailed meteorological analysis of each STT event is presented and observations are interpreted with the Realtime Air Quality Modeling System (RAQMS). The implications of the two STT events are discussed in terms of the impact on the total tropospheric O_3 budget and the impact on air quality and policy-making.

1 Introduction

Stratosphere-to-troposphere transport (STT) contributes to and alters the trace gas composition of the troposphere and as such STT has been extensively studied for over 50 yr (e.g. Danielsen, 1968; Danielsen and Mohnen, 1977; Lamarque and Hess, 1994; Thompson et al., 2007; Lefohn et al., 2011). Ozone (O_3) is present in large quantities in the stratosphere compared to the troposphere and is commonly used as a tracer for STT. In the free troposphere, air masses of stratospheric origin can be transported and mixed with tropospheric air masses, contributing to the topospheric O_3 budget. Understanding the dynamic processes that control the tropospheric O_3 budget is of importance not only for understanding surface air quality in areas affected by STT, but also because upper tropospheric O_3 is an important greenhouse gas affecting outgoing long-wave radiation (Worden et al., 2008) and impacting surface temperature (IPCC, 2007).

Tropopause folds and cut-off lows have been identified as the most important mechanisms to cause STT and have subsequently been the focus of STT investigations (e.g. Danielsen and Mohnen, 1977; Ebel, 1991; Vaughan, 1994; Bonasoni, et al., 2000; Søensen and Nielson, 2001; Lefohn et al., 2011). Evidence of stratospheric O_3 intrusions within the free troposphere have been reported in long-term data-sets from mountain-top O_3 measuring sites (e.g. Bonasoni et al., 2000; Stohl et al., 2000) and from aircraft and ozonesondes (e.g. Zanis et al., 2003; Cooper et al., 2005; Bowman et al., 2007; Bourqui and Trepainer, 2010). STT events are episodic in nature with peak episodes occurring during the winter-spring period; the frequency and magnitude of STT events are important factors in understanding the possible degree to which they affect surface and free troposphere O_3 mixing ratios (Lefohn et al., 2011).

Identifying STT within the tropospheric boundary layer, especially at near-sea-level surface sites, is challenging. The stratospheric characteristics (high O_3, low humidity) may be lost by the time this air is entrained into the boundary layer, making STT difficult to diagnose. In addition, the O_3 mixing ratio within STT events is expected to be highly variable depending on the stratospheric origin and degree of mixing in the free troposphere. Although evidence of STT at sea-level surface sites has been presented (Langford et al., 2012; Lefohn et al., 2012; Lin et al., 2012; Chung and Dann, 1985) the magnitude of the effects of STT on boundary layer O_3 mixing ratios is still under debate (Lefohn et al., 2011; Langford et al., 2009; Lin et al., 2012; Fiore et al., 2003).

The United States Environmental Protection Agency (EPA) sets National Ambient Air Quality Standards (NAAQS) for ground-level O_3 which are used to assess air quality. The 2008 NAAQS for O_3 requires that the 3 yr average of the annual 4th-highest daily maximum 8 h mean mixing ratio be less than or equal to 75 ppbv (parts per billion by volume) (US EPA, 2006), with a decision on the proposed reduction of the NAAQS O_3 target to 60–70 ppbv due in 2014 (US EPA, 2010). The formulation of the NAAQS O_3 standard relies on the accurate identification of a representative background mixing ratio of O_3 that would occur in the United States in the absence of anthropogenic contributions. Current background O_3 mixing ratios are estimated to be in the range of 15–35 ppbv (Langford et al., 2009), contributing up to 47 % towards the current NAAQS O_3 target of 75 ppbv. Some studies have reported higher background O_3 mixing ratios, particularly in springtime, suggesting that STT has a significant influence on the background O_3 mixing ratios (Cooper et al., 2005; Hocking et al., 2007; Lefohn et al., 2011; Langford et al., 2012; Lin et al., 2012). If the proposed reduction of NAAQS O_3 target is approved, the identification of STT and evidence of its contribution towards background O_3 mixing ratios will become increasingly important, as the gap between background O_3 and the NAAQS O_3 target is reduced.

The western United States, due to its location at the end of the North Pacific mid-latitude storm track, has been identified as a preferred location for deep STT reaching below 700 mbar (Sprenger and Wernli, 2003). Understanding the boundary conditions coming into the western United States is important for air quality issues, however large areas in the western United States have limited or no O_3 data. In addition, the existing positive vertical gradient for O_3, complex mountainous terrain of the Western United States and resulting meso-scale dynamics, further complicate efforts to model O_3 concentrations.

In this paper, detailed analysis of two STT events occurring during spring 2012 over California, USA is presented. This work reports airborne in situ measurements of O_3 and other trace gases and a discussion of the meteorological conditions leading to STT. Evidence of the use of a non-traditional stratospheric tracer (carbon dioxide, CO_2)

ACPD
13, 10157–10192, 2013

which can be used in conjunction with O_3 to help with the identification and interpretation of STT events is also presented. Observations are interpreted with Realtime Air Quality Modeling System (RAQMS). Finally, the implications of the two STT events are discussed in terms of the impact on air quality and policy-making.

2 Experimental approach

2.1 Airborne instrumentation

In situ measurements of O_3 vertical profiles were carried out onboard the Alpha Jet research aircraft as part of the Alpha Jet Atmospheric eXperiment (AJAX). The aircraft is based at and operated from NASA Ames Research Center at Moffett Field, CA (37.415° N, 122.050° W). Scientific instrumentation is housed within one of two externally mounted wing-pods, each of which has a maximum payload weight of 136 kg. The aircraft was flown with one instrumented wing-pod attached, containing an O_3 monitor (described below) and a CO_2 analyzer (Picarro Inc., model G2301-m), details of which are reported by Tadić et al. (2013). The aircraft also carries GPS and inertial navigation systems that provide altitude, temperature and position information time stamped with coordinated universal time (UTC) for each research flight.

Measurements of O_3 mixing ratios were performed using a commercial O_3 monitor (2B Technologies Inc., model 205) based on ultraviolet (UV) absorption techniques and modified for flight worthiness. The dual-beam instrument uses two detection cells to simultaneously measure UV light intensity differences between O_3-scrubbed air and un-scrubbed air to give precise measurements of O_3. The monitor has been modified by upgrading the pressure sensor and pump to allow measurements at high altitudes, including a lamp heater to improve the stability of the UV source, and the addition of heaters, temperature controllers and vibration isolators to control the monitor's physical environment.

ACPD
13, 10157–10192, 2013

The air intake is through Teflon tubing (perfluroalkoxy-polymer, PFA) with a backward-facing inlet positioned on the underside of the instrument wing pod. Air is delivered through a 5 µm PTFE (polytetrafluroethylene) membrane filter to remove fine particles prior to analysis.

The O_3 monitor has undergone thorough instrument testing in the laboratory to determine the precision, linearity and overall accuracy. Eight-point calibration tests (ranging from 0–300 ppbv) were performed before and after each flight using an O_3 calibration source (2B Technologies, model 306 referenced to the WMO scale). Calibration settings for the O_3 monitor were left at manufacturer default settings and corrections to account for linearity offset and zero-offset were applied during data processing. For the flights reported here, the linearity offset was determined to be 1.01 and the zero-offset was −2.4 ppbv.

Calibrations in a pressure- and temperature-controlled environmental chamber were performed using the O_3 calibration source over the pressure range 200–800 mbar and temperature range −15 to +25 °C; typical pressure and temperature ranges observed in the wing-mounted instrument pod during flight. Precision during chamber tests, determined from the standard deviation when sampling O_3 mixing ratios of 50 ppbv over 2 min duration and during simulated descent profiles, was found to be 2 ppbv. The zero-offset, observed when sampling O_3-scubbed air during simulated descent profiles was found to linearly increase by 0.6 ppbv with decreasing chamber pressure (typical zero-offset of −2.4 ppbv at ground level and −3 ppbv at 200 mbar). Instrument drift estimated based on 1 h of sampling 50 ppbv O_3 was 1.5 ppbv.

The in situ measurements were carried out over the San Joaquin Valley, CA (SJV), (Castle airport, Merced: 37.381° N, 120.568° W) and offshore (RAINS Intersection: 37.169° N, 123.235° W). Take-off time from Moffett Field was at 18:00 UTC on 14 May 2012 and 5 June 2012. The aircraft arrived on-station at the SJV site at 18:20 UTC (local time is UTC – 7 h) on each day and performed a descending spiral-profile from ∼ 8.8 km to < 0.5 km with a descent rate of ∼ 370 m min^{-1}. A second descending spiral-profile was performed over the offshore location starting at 19:05 UTC on 14 May 2012, from ~8.5 km to 1.5 km; the aircraft was prevented from flying any lower on this day due to a thick marine stratus layer with a top at 1.5 km. The lowest altitude of the offshore profile on 5 June 2012 was < 0.5 km. Total flight time each day was 100 min.

2.2 RAQMS model description

Global in-line O_3 and meteorological forecasts from the Real-time Air Quality Modeling System (RAQMS) (Pierce et al., 2007, 2009) are used in conjunction with Reverse Domain Filling (RDF) techniques (Sutton et al., 1994; Fairlie et al., 2007) to provide a large scale context for the interpretation of the STT events and to assess the fidelity of the RAQMS O_3 forecasts. Forecasts are initialized with satellite based O_3 analyses and are archived at 6 h intervals at a horizontal resolution of $1^\circ \times 1^\circ$ with 35 hybrid eta-theta vertical levels extending from the surface to approximately 60 km. Stratospheric O_3 analyses are constrained through assimilation of near-real-time (NRT) O_3 profiles from the Microwave Limb Sounder (MLS) (Waters et al., 2006) above 50 mbar and NRT cloud cleared total column O_3 retrievals from the O_3 Monitoring Instrument (OMI) (Levelt et al., 2006). The RAQMS dynamical core is the University of Wisconsin (UW) hybrid isentropic–eta coordinate (UW Hybrid) model (Zapotocny et al., 1997; Schaack et al., 2004). Meteorological forecasts are initialized with operational analyses from the National Centers for Environmental Prediction (NCEP) Global Data Assimilation System (GDAS) (Kleist et al., 2009). 6 h chemical and meteorological forecasts provide chemical and meteorological input for the RDF calculations. Analyzed O_3 results are plotted as curtains along the flight track for comparison to the in situ data.

The RDF technique has been shown to represent coarsely resolved constituent fields at higher resolution, with higher information content, than originally observed (Sutton et al., 1994) or modeled (Fairlie et al., 2007). The RAQMS RDF calculations are based on analysis of back trajectories initialized along the aircraft flight track. Three-dimensional 6 day back trajectory calculations were conducted using the Langley Trajectory Model (LTM) (Pierce and Fairlie, 1993; Pierce et al., 1994). Back trajectories are initialized at model hybrid levels every 5 min along the flight track to construct a curtain.

ACPD
13, 10157–10192, 2013

The back-trajectories sample and archive RAQMS chemical and dynamical quantities so that Lagrangian averages could be determined. The Lagrangian averages are then mapped back onto the initial flight curtain to produce the RDF products. For the STT analysis we focus on RDF O_3, large-scale mixing efficiency, and continental PBL exposure.

3 Results and discussion

3.1 A cut-off low event: 14 May 2012

The flight profile and O_3 mixing ratios encountered along the 14 May 2012 flight are presented in Fig. 1. Anomalously high O_3 mixing ratios > 120 ppbv are found between 5 and 7 km, (600 to 400 mbar) with a maximum of 150 ppbv, creating a steep O_3 gradient between the free troposphere and boundary layer.

The high O_3 mixing ratios were sampled inside a cut-off low pressure system. The cut-off low is associated with relatively strong isentropic potential vorticity (PV) and high O_3 extending from the lower stratosphere into the mid-troposphere. PV is a conservative tracer under adiabatic conditions and is typically much larger in the stratosphere than troposphere; as such cross-sections of PV indicate descent of stratospheric airmasses into the troposphere. Figure 2 shows the 5 km maps and 122° W cross-sections of enhanced O_3 and PV at 18:00 UTC on 14 May 2012.

Figure 3 shows the in situ measurements of potential temperature and dew point (Fig. 3a) and O_3, CO_2 and water vapor (Fig. 3b, c). Potential temperature and dew point are taken from the most proximal radiosonde launches (Oakland (OAK)) and clearly identify a stable layer at 800 mbar which existed before (dotted lines) and persisted after (solid lines) the time of the aircraft measurements. A pronounced dry, stable layer is present at 500 mbar in the radiosonde sounding taken ~ 5 h after aircraft measurements, identifying the vertical extent of the stratospheric intrusion. This was not evident in the preceding radiosonde sounding as at that time the center of the cut-off low was still located to the west of OAK.

The O_3, CO_2 and water vapor mixing ratios observed during each profile are shown in Fig. 3b (offshore) and Fig. 3c (SJV). CO_2 is a non-conventional tracer of stratospheric air and provides an interesting comparison between stratospheric and tropospheric air masses. A clear increase in O_3 and decrease in CO_2 and water vapor mixing ratios is observed between 600–400 mbar in the offshore profile and between 800–500 mbar above the SJV. These perturbations are more pronounced in the offshore profile, compared to the SJV profile where the intrusion is vertically spread and as such has a slightly lower overall maximum O_3 mixing ratio. However, the O_3 maximum and CO_2 and water vapor minima in both profiles is located near 550 mbar.

CO_2 can be viewed as a more inert tracer than O_3, since it has no known sinks in the lower stratosphere (Aoki et al., 2003). The seasonal cycle of tropospheric CO_2 has a large amplitude characterized by a maximum in spring (April/May in the Northern Hemisphere) and minimum in summer (July) (Sawa et al., 2008; Hoor et al., 2004; Boering et al., 1996; Nakazawa et al., 1991). In the lower stratosphere CO_2 has a less pronounced seasonal cycle with low concentrations in spring and higher concentrations in summer. From the seasonal cycle information presented by Sawa et al. (2008) we expect stratospheric CO_2 mixing ratios during the time of this study (May–early June) to be less than tropospheric CO_2 mixing ratios, as observed within the STT on 14 May 2012. As such, at this time of year in the Northern Hemisphere, CO_2 measurements collocated with O_3 and water vapor can be used as tracers of STT events. The use of additional tracers, such as CO_2, further confirms the intrusion to be stratospheric in nature as opposed to aged and lofted Asian pollution, where CO_2 mixing ratios would be expected to be representative of tropospheric values.

Figure 4 shows results of the RAQMS RDF curtain calculations for this flight along with the analyzed O_3 curtain (as described in Sect. 2.1). The RAQMS RDF O_3 shows a much sharper vertical gradient in the upper troposphere than the analyzed O_3 with RDF O_3 in excess of 120 ppbv below and 60 ppbv above 8 km. To determine which

ACPD
13, 10157–10192, 2013

parts of the flight curtain may have been exposed to air within the continental planetary boundary layer (PBL) we track the amount of time each back trajectory spent within the continental PBL and then use 7 day (7–14 May 2013) averaged total column carbon monoxide (CO) from the Atmospheric InfRared Sounder (AIRS) (Aumann and Miller, 1995) to distinguish between exposure to clean and polluted continental PBL air. An AIRS total column CO threshold of 2.5×10^8 mol cm^{-2} was used distinguish between clean and polluted continental boundary layer exposure. By monitoring the amount of time that the back trajectories spent within either clean or polluted continental (PBL) we can see that, on average, the airmass above the STT event spent about 40 % of its time within a clean continental boundary layer. The RAQMS RDF calculations predict no exposure to polluted continental boundary layer air along the aircraft flight track (not shown), which is consistent with the observed CO_2.

The RDF mixing curtain provides a measure of the efficiency of large-scale mixing along the back trajectories and is determined from the Lagrangian averaged rate of stretching of air parcels (Haynes, 1990; Fairlie et al., 2007). Regions of large positive RDF mixing (warm colors) are associated with strong shear flow where neighboring air parcels can mix efficiently. Regions of large negative RDF mixing (cool colors) are associated with rotational flow, where air parcels tend to remain more isolated. After 18:36 UTC, the 14 May 2012 STT event is associated with efficient large-scale mixing along the southern flank of the cut-off low, which leads to stretching of the air parcels and generation of laminar ozone features. Prior to 18:36 UTC and below 6 km the RDF mixing is negative, indicating that the air parcels have remained relatively isolated. This portion of the RDF curtain is within the rotational flow associated with the cut-off low (see Fig. 2).

This STT encounter provides an opportunity to evaluate the ability of the RAQMS O_3 analysis and RAQMS RDF O_3 to capture the observed structure of the O_3 intrusion and to assess the influence of numerical diffusion on predicted transport of stratospheric air into the troposphere. Figure 5 shows comparisons between the in situ O_3 measurements, RAQMS O_3 analyses, and RAQMS RDF O_3 along the aircraft flight track. The

ACPD
13, 10157–10192, 2013

first encounter with the STT event occurs prior to 18:30 UTC during the descending portion of the onshore profile. During this flight leg both the RAQMS analyzed and RDF O_3 overestimate the observed O_3 mixing ratio but the RDF O_3 captures the sharp vertical variations much better than the analyzed O_3. Between 18:30 UTC and 18:48 UTC the aircraft descends below 6 km and then begins to ascend again. During this time period, when the aircraft is sampling within the cut-off low and the air is isolated from large-scale mixing, both the RAQMS RDF and analyzed O_3 are in relatively good agreement with the in situ O_3. Between 18:48 UTC and 19:12 UTC the aircraft completes the ascending portion of the onshore profile, reaches maximum altitude, and conducts the descending portion of the offshore profile. During these legs the aircraft penetrates through the STT event twice, with in situ O_3 ranging from 120 ppbv to 140 ppbv within the STT and 60 ppbv above. The RDF O_3 does a very good job in capturing this variation while the analyzed O_3 shows a much broader O_3 peak. The narrow O_3 lamina captured by the RDF O_3 analysis is poorly resolved because of the relatively coarse horizontal and vertical resolution of RAQMS. As the scale of the O_3 lamina approaches the RAQMS grid dimensions numerical diffusion becomes very large and the narrow feature is lost. After 19:12 UTC the aircraft is again below 6 km and within the cut-off low where rotational flow dominates and both the RDF and analyzed O_3 are in good agreement with the in situ measurements.

The RAQMS back trajectories can be used to identify the origin of the high (> 120 ppbv) RDF O_3 predicted within the STT event. Figure 6 shows the back trajectory history and origin of the high (> 120 ppbv) RDF O_3 mixing ratios beginning on 18:00 UTC on 8 May 2012, 6 days prior to being sampled by the aircraft. The underlying map on the left side of Fig. 6 shows 7 day averaged total column O_3 from AIRS during the period from 7–14 May 2012. The back trajectories show a significant amount of dispersion over the previous 6 days, with meridional spread in the back trajectories within the first 2–3 days and longitudinal spread 3–6 days prior to sampling by the aircraft. The majority of the high RDF O_3 along the aircraft curtain originated to the south of a region of high mean column O_3 off the coast of Asia 6 days prior to sampling. The

Discussion Paper | Discussion Paper | Discussion Paper | Discussion Paper |

ACPD
13, 10157–10192, 2013

Springtime stratosphere-to-troposphere transport

E. L. Yates

origin of the STT event is an elongated region extending north eastward from South Korea over Southern Japan to about 45° North at the International Date line. The right side of Fig. 6 shows the RAQMS analyzed O_3 and zonal wind 135° E cross-section at 18:00 UTC on 8 May 2012. The cross-section shows that the STT event originated between 10–12 km on the northern flank of a strong (> 60 m s^{-1}) westerly jet. There are strong meridional gradients in O_3 across the jet axis, with high stratospheric O_3 on the poleward and lower O_3 on the equatorward side of the jet. Analysis of the STT back trajectories at 18:00 UTC on 8 May 2012 shows that mean O_3 mixing ratio at the origin of the STT event is 163 ppbv with a standard deviation of 50 ppbv. Efficient large-scale mixing of this initial distribution with lower mixing ratio O_3 within the troposphere as well as numerical diffusion results in reductions in the mean and standard deviation in the analyzed STT to 97 ppbv and 7.5 ppbv, respectively when it is sampled by the aircraft on 14 May 2012.

3.2 A post-trough, building ridge event: 5 June 2012

A deep, late-season extra-tropical cyclone affected California on 5 June 2012 and injected stratospheric air into the troposphere. The STT event observed on 5 June 2012 was more pronounced, when comparing maximum O_3 mixing ratios in each STT event, than the event on 14 May 2012. Anomalously high O_3 mixing ratios were observed between 3 and 4 km (750 to 600 mbar) creating a steep ozone gradient between the intrusion (up to 120 ppbv offshore and 200 ppbv over SJV) and surrounding air masses (40 and 50 ppbv offshore and over SJV respectively).

Figure 7 shows 4 km maps and 120° W cross-sections of RAQMS O_3 and PV at 18:00 UTC on 5 June 2012. An extensive region of enhanced O_3 and PV over central California at 4 km is being advected in from the Northwest behind the trough. The RAQMS analyzed O_3 is greater than 80 ppbv and PV is in excess of 1.5 PVU indicating stratospheric air. This enhanced O_3 and PV extends down into the troposphere along the northern flank of a relatively strong (45 m s^{-1}) jet at 120° W. The aircraft flight path

ACPD
13, 10157–10192, 2013

intersects the high O_3 and PV during the SJV profile and appears to be just to the south of the enhancement at 4 km during the off-shore spiral.

Radiosonde launches from OAK observed the stratospheric intrusion as a dry stable region (Fig. 8a) near 650 mbar in the 5 June 2012 12:00 UTC radiosonde sounding (dotted lines) and at 700 mbar in the 6 June 2012 00:00 UTC radiosonde sounding (solid lines). O_3, CO_2 and water vapor mixing ratios observed during each profile are shown in Fig. 8b (offshore) and Fig. 8c (SJV). O_3 increases between 750–600 mbar in both profiles; an O_3 maximum in both instances is observed at 640 mbar. The O_3 increase is more pronounced in the SJV profile, compared to the offshore location. Also, in both profiles there are decreases in CO_2 and water vapor mixing ratios at the same pressures as the O_3 increases, corroborating the assignment of stratospheric origin.

Figure 9 shows results of the RAQMS RDF curtain calculations for this flight along with the analyzed O_3 curtain. The RDF and analyzed O_3 both show STT O_3 enhancements near 4 km during the first half of the flight (SJV profile) although the RDF O_3 shows sharper gradients and higher (> 100 ppbv) mixing ratios than the analyzed O_3. Neither RDF or analyzed O_3 show significant enhancements during the latter half of the flight (offshore profile) with peak O_3 mixing ratios generally less than 70 ppbv at 3–4 km. The RDF mixing curtain shows that the lower half of the STT event is associated with negative mixing efficiencies, indicating that this air has remained relatively isolated during the previous 6 days. The RDF continental PBL exposure curtain shows that the STT event has not been exposed to the continental PBL during the previous 6 days but the low O_3 air immediately above and below the STT event has spent more than 75 % of its time within a clean continental boundary layer before being sampled by the aircraft.

Figure 10 shows comparisons between the in situ O_3 measurements, RAQMS O_3 analyses, and RAQMS RDF O_3 along the aircraft flight track. The aircraft samples the STT event three times prior to 19:00 UTC. During this period the RDF O_3 shows narrower features and somewhat higher mixing ratios than the analyzed O_3 but neither is able to capture the amplitude of the observed O_3 peak which is greater than 150 ppbv during each of the three encounters and reaches 190 ppbv at 18:42 UTC during the SJV spiral. The aircraft is above the STT event between the first and second STT encounters, and the RDF O_3 captures the sharp vertical gradients and shows generally better agreement with the in situ measurements. The aircraft is below the STT event between the second and third STT encounters, and both RDF and analyzed O_3 are in good agreement with the in situ measurements. The aircraft encounters the STT event once at 19:30 UTC during the offshore profile with both RDF and analyzed O_3 showing significant underestimates in O_3. Between 19:36 and 19:48 UTC the aircraft samples marine boundary layer where both the RDF and analyzed O_3 are in good agreement with the in situ measurements. The STT event is sampled for the fifth time between 19:54 and 20:00 UTC and both RDF and analyzed O_3 capture the observed vertical gradient, but miss the high O_3 within the STT by up to 50 ppbv.

The RAQMS back trajectories are used to identify the origin of the relatively high (> 80 ppbv) RDF O_3 predicted within the onshore part STT event. Figure 11 shows the back trajectory history and origin of the high (> 80 ppbv) RDF O_3 mixing ratios beginning on 18:00 UTC on 30 May 2012, 6 days prior to being sampled by the aircraft. The underlying map on the left side of Fig. 11 shows 7 day averaged total column O_3 from AIRS during the period from 29 May–5 June 2012. During the first day prior to being sampled by the aircraft the STT back trajectories remain very compact and move northwestward into a region South of Alaska with high AIRS average total column O_3. Three days prior to being sampled by the aircraft some of the STT back-trajectories are dispersed further westward into the region of high AIRS average total column O_3 over Japan and Siberia. However, the majority of the STT back trajectories remain south of Alaska and circulate within a large, stationary low pressure system near 150° W. The right side of Fig. 11 shows the RAQMS analyzed O_3 and zonal wind 150° W cross-section at 18:00 UTC on 30 May 2012. The STT trajectories originated within the core of the stationary low pressure system in a region of moderately high O_3 and low wind speeds between 6–8 km. Analysis of the STT back trajectories at 18:00 UTC on 30

ACPD
13, 10157–10192, 2013

May 2012 shows that mean O_3 mixing ratios at the origin of the STT event is 102 ppbv with a standard deviation of 14 ppbv, both of which are significantly lower then found within the origin of the 14 May 2012 STT encounter. The low initial variance of the 5 June 2012 STT trajectories, combined with the fact that this STT encounter was associated with relatively isolated air and weak large-scale mixing, accounts for the smaller differences between the RDF and analyzed O_3 for this flight and indicates that processes other than large-scale shear lead to the narrow STT event observed on this flight. It is possible that inertial gravity wave transport could have contributed given the close proximity of the flight to a strong jet core (see Fig. 11).

3.3 Stratosphere-to-troposphere implications

To assess the contribution of the two STT events on the tropospheric O_3 budget, total tropospheric O_3 for each STT event was calculated in Dobson Units (DU) based upon the summation of the tropospheric O_3 (below ~ 9 km (365 mbar)) normalized by dividing by the thickness (mbar) of the atmosphere over which O_3 measurements were taken (DU/100 mbar) following the method of Cooper et al. (2011). The STT event on 14 May 2012 has a greater total tropospheric O_3 DU/100 mbar value compared to the 5 June 2012 event, even though the 14 May 2012 STT event had a reduced maximum O_3 mixing ratio compared to 5 June 2012. This is because the stratospheric intrusion on 14 May 2012 was more vertically extensive compared to the fine filament structure observed during the 5 June 2012 STT, resulting in a larger overall enhancement of total tropospheric O_3.

For 14 May 2012, total tropospheric O_3 in DU/100 mbar was 6.5 DU/100 mbar in the offshore profile and 6.9 DU/100 mbar above the SJV, compared to 4.2 and 3.8 DU/100 mbar in the offshore and SJV profiles respectively on 5 June 2012. For comparison, these values are within the range observed during the IONS-2010 campaign in May–June 2010 reported by Cooper et al. (2011), where typical values were within the range of 2–7 DU/100 mbar. Given the importance of upper tropospheric O_3 in terms of its radiative qualities and the fact that some STT events, particularly narrow

ACPD
13, 10157–10192, 2013

intrusions, may be difficult to detect by means other than in situ methods, for example by total tropospheric O_3 column satellite retrievals, this work highlights the importance of routine collection of in-situ measurements of tropospheric O_3 to better understand the frequency, magnitude and controlling processes of STT.

The US EPA can currently exclude from the NAAQS O_3 target any surface O_3 monitoring data identified as being influenced by an extreme stratospheric intrusion, since the naturally occurring "exceptional events" are uncontrollable by State agencies. However, identification of STT contributing to surface O_3 sites remains challenging for several reasons, including a lack of vertical O_3 measurements which identify the extent of the intrusion, and the limited effectiveness of models in forecasting the impacts of STT in part due to the complex topography of the western United States and resulting meso-scale dynamics (e.g. mountain lee waves and low-level jets). Furthermore, stratospheric intrusions can remain aloft or contribute to the overall background by gradual mixing with the boundary layer making a distinct O_3 enhancement difficult to distinguish, and the effects of a stratospheric intrusion may result in an increase of O_3 at a surface site during daytime when photochemical processing further complicates identification. The two STT events analyzed here intrude down to 800–500 mbar on 15 May 2012 and 750–600 mbar on 5 June 2012, both of which are deep enough to potentially be entrained into the boundary layer and impact surface sites, particularly when considering the mountainous terrain of the western United States and convection during springtime, both of which intensify vertical mixing.

Maps of the US EPA air quality index from 5–6 June 2012 showed moderate to high O_3 over parts of California, Nevada, Utah and Wyoming, with exceedances of the NAAQS O_3 standard in southwestern Utah, eastern Nevada and Wyoming (http://www.airnow.gov). Potential vorticity and O_3 from the 18:00 UTC RAQMS analysis for 5 June 2012 also shows how the stratospheric intrusion descends to low altitudes (< 4 km) over California, Nevada, Utah and east to 111° W. To further investigate the possibility of STT contributing to surface-level O_3, 1 h O_3 mixing ratios were obtained

ACPD
13, 10157–10192, 2013

from rural sites in Grand Canyon National Park, Arizona (GC), Great Basin National Park, Nevada (GB), South Pass, Wyoming (WY) and Zion National Park, Utah (ZN).

Assessment of STT impacts on surface sites for the 14 May 2012 STT event proved difficult. Air quality maps from 14 May 2012 show enhanced O_3 over southern California, southern and eastern Nevada, Arizona and Utah. Timeseries plots of the one-hour surface O_3 from GB, ZN and GC show a general increase in the diurnal cycle of surface O_3 during 15–16 May 2012 compared to the days before and after, however, there is no distinct enhancement outside of the daytime periods, making the potential contribution from STT difficult to assess (see Fig. 12a).

Enhancements of surface O_3 are observed during 5–6 June 2012 (see Fig. 12b). Maximum surface O_3 enhancements at GB and ZN occur on 5 June 2012 reaching 79 ppbv at 16:00 LT at GB and 85 ppbv at 19:00 LT at ZN. However, the occurrences during daytime hours complicate identification of STT influence at these sites. In the WY site, a distinct increase in O_3 is observed with a maximum of 91 ppbv measured at 00:00 LT on 6 June 2012. This is clearly not a result of photochemical processing and as such is most likely evidence of the impact of STT at surface sites.

4 Conclusions

The difference in the trace gas composition of the stratosphere compared to the troposphere permits the identification of air masses of stratospheric origin found within the free troposphere occurring during STT events. In this paper we presented two STT case studies sampled over California: one on 14 May 2012 associated with a cut-off low and one on 5 June 2012 occurring in a post-trough, building ridge event.

In each case, high O_3 was measured within the stratospheric intrusion at altitudes as low as 3 km. During both events the stratospheric air was characterized by high O_3 and low water vapor and CO_2 mixing ratios. The observation of decreased CO_2 within the stratospheric air mass is consistent with the varying seasonal cycles of CO_2 in the

ACPD
13, 10157–10192, 2013

troposphere and stratosphere and provides evidence and support for the use of in situ carbon dioxide measurements as an additional method for detecting STT events.

RAQMS O_3 analysis and RDF diagnostics provide a large-scale context for the interpretation of the airborne measurements. RDF results show that the two STT events had very different airmass histories. The 14 May 2012 STT event was associated with a cut-off low pressure system that moved into central California from the southwest and experienced efficient large-scale mixing during the previous 6 days. As a result, this STT event was composed of air with origins that extended over a wide longitudinal range with considerable initial variability in O_3 mixing ratios. In contrast, the 5 June 2012 STT had its origins within the core of a large, stationary low pressure system over the Gulf of Alaska and remained relatively isolated with very little large-scale mixing during the previous 6 days. Comparisons between the in situ O_3 and RAQMS RDF and analyzed O_3 along the flight track show that the RDF O_3 was able to do a very good job in capturing the high ozone within the 14 May 2012 STT event while the analyzed O_3 was not able to maintain the strong vertical gradients that were observed. This was attributed to increasing numerical diffusion as the scale of the STT event approached the model grid scale. Neither the RDF or analyzed O_3 was able to capture the high O_3 observed during the 5 June 2012 STT event, suggesting that the high O_3 within very narrow O_3 lamina may be due to inertial gravity wave transport, which neither analyzed or RDF O_3 are able to represent.

The impact of the two STT events on the tropospheric O_3 budget has been assessed by comparing the total tropospheric O_3 (DU) from each analysis day. The STT event on 14 May 2012, although displaying a smaller O_3 maximum mixing ratio, had a greater total tropospheric O_3 DU value than the 5 June 2012 STT event. The fine filament structure of the STT on 5 June 2012 makes it difficult to detect the STT event from a total tropospheric O_3 column measurement alone. This work highlights the importance of in situ measurements in the detection of STT, which in some cases may be the only way to accurately detect and analyze different occurrences of STT.

ACPD
13, 10157–10192, 2013

Investigations were conducted to assess the potential impacts of the STT events on rural surface O_3 monitoring sites. Evidence supporting STT influence on monitoring sites was detected, with a particular O_3 episode exceeding NAAQS O_3 standard measured at South Pass, Wyoming likely associated with the observed STT on 5 June 2012. More quantitative support for the STT influence on surface O_3 requires additional airborne measurements and multi-scale, nested modeling approaches. This study has shown that the RAQMS global O_3 analyses underestimate the high O_3 mixing ratios observed in both STT events. As a result, higher resolution modeling studies using global scale O_3 analyses for lateral boundary conditions likely underestimate the magnitude of the exceedances due to STT. Preliminary comparisons between South Pass Wyoming surface O_3 observations and predictions from nested RAQMS/WRF-CHEM 8 km simulations of the June STT event confirm this.

Acknowledgements. The authors gratefully recognize the support and partnership of H211 L. L. C., with particular thanks to K. Ambrose, R. Simone, B. Quiambao, J. Lee, J. McMahon and R. Fischer. Funding was provided by the NASA Postdoctoral Program (J. T.), San Jose State University Research Foundation (E. Y.), and the Bay Area Environmental Research Institute (M. R.). Funding for instrumentation and aircraft integration is gratefully acknowledged from Ames Research Center Director's funds. Helpful discussions with R. S. Hipskind, P. Hamill, L. Pfister and R. Chatfield are happily acknowledged. Technical contributions from Z. Young, E. Quigley, R. Walker, and A. Trias made this project possible. The views, opinions, and findings contained in this report are those of the author(s) and should not be construed as an official National Oceanic and Atmospheric Administration or US Government position, policy, or decision.

References

Aumann, H. H. and Miller, C.: Atmospheric Infrared Sounder (AIRS) on the Earth observing system, SPIE, 2583, 32–343, doi:10.1117/12.228579, 1995.

Aoki, S., Nakazawa, T., Machida, T., Sugawara, S., Morimoto, S., Hashida, G., Yamanouchi, T., Kawamura, K., and Honda, H.: Carbon dioxide variations in the stratosphere over Japan,

ACPD
13, 10157–10192, 2013

Scandinavia and Antarctica, Tellus B, 55, 178–186, doi:10.1034/j.1600-0889.2003.00059.x, 2003.
Bonasoni, P., Evangelisti, F., Bonafe, U., Ravegnani, F., Calzolari, F., Stohl, A., Tositti, L., Tubertini, O., and Colombo, T.: Stratospheric ozone intrusion episodes recorded at Mt. Cimone during the VOTALP project: case studies, Atmos. Environ., 34, 1355–1365, 2000.
Bourqui, M. S. and Trépanier. P.-Y.: Descent of deep stratospheric intrusions during the IONS August 2006 campaign, J. Geophys. Res., 115, D18301, doi:10.1029/2009JD013183, 2010.
Bowman, K. P., Pan, L, L., Campos, T., and Gao, R.: Observations of fine-scale transport structure in the upper troposphere from the High-performance Instrumented Airborne Platform for Environmental Research, J. Geophys. Res., 112, D18111, doi:10.1029/2007JD008685, 2007.
Chung, Y. S. and Dann, T.: Observations of stratospheric ozone at the ground level in Regina, Canada., Atmos. Environ., 19, 157–162, doi:10.1016/0004-6981(85)90147-7, 1985.
Cooper, O. R., Stohl, A., Hübber, G., Hsie, E. Y., Parrish, D. D., Tuck, A. F., Kiladis, G. N., Oltmans, S. J., Johnson, B. J., Shapiro, A., Moody, J. L., and Lefohn, A. S.: Direct transport of midlatitude stratospheric ozone into the lower troposphere and marine boundary layer of the tropical Pacific Ocean, J. Geophys. Res., 110, D23310, doi:10.1029/2005JD005783, 2005.
Cooper, O. R., Oltmans, S. J., Johnson, B. J., Brioude, J., Angevine, W., Trainer, M., Parrish, D. D., Ryerson, T. R., Pollack, I., Cullis, P. D., Ives, M. A., Tarasick, D. W., Al-Saadi, J., and Stajner, I.: Measurement of western US baseline ozone from the surface to the tropopause and assessment of downwind impact regions, J. Geophys. Res., 116, D00V03, doi:10.1029/2011JD016095, 2011.
Danielsen, E. F.: Stratospheric-tropospheric exchange based on radioactivity, ozone and potential vorticity, J. Atmos. Sci., 25, 502–518, 1968.
Danielsen, E. F. and Mohnen, V. A.: Project duststorm report: ozone transport, in-situ measurements, and meteorological analysis of tropopause folding, J. Geophys. Res., 82, 5867–5877, doi:10.1029/JC082i037p05867, 1977.
Ebel, A., Hass, H., Jakobs, H. J., Laube, M., Memmesheimer, M., Oberreuter, A., Geiss, H., and Kuo, Y.-H.: Simulation of ozone intrusion caused by a tropopause fold and cut-off low, Atmos. Environ., 25, 2131–2144, 1991.
Fairlie, T. D., Avery, M. A., Pierce, R. B., Al-Saadi, J., Dibb, J., and Sachse, G.: Impact of multiscale dynamical processes and mixing on the chemical composition of the upper troposphere

and lower stratosphere during the Intercontinental Chemical Transport Experiment–North America, J. Geophys. Res., 112, D16S90, doi:10.1029/2006JD007923, 2007.
Fiore, A., Jacob, D. J. Liu, H., Yantosca, R. M., Fairlie, T. D., and Li, Q.: Variability in surface ozone background over the United States: implications for air quality policy, J. Geophys. Res., 108, 4787, doi:10.1029/2003JD003855, 2003.
Hocking, W. K., Carey-Smith, T., Tarasick, D. W., Argall, P. S., Strong, K., Rochon, Y., Zawadzki, I., and Taylor, P. A.: Detection of stratospheric ozone intrusions by windprofiler radars, Nature, 450, 281–284, 2007.
Hoor, P., Gurk, C., Brunner, D., Hegglin, M. I., Wernli, H., and Fischer, H.: Seasonality and extent of extratropical TST derived from in-situ CO measurements during SPURT, Atmos. Chem. Phys., 4, 1427–1442, doi:10.5194/acp-4-1427-2004, 2004.
IPCC (Intergovernmental Panel on Climate Change, Climate Change): The Physical Science Basis, Summary for Policymakers – Contribution of Working Group I to the Fourth Assessment Report of the Intergovernmental Panel on Climate Change, Cambridge University Press, New York, 2007.
Kleist, D. T., Parrish, D. F., Derber, J. C., Treadon, R., Wu, W.-S., and Lord, S.: Introduction of the GSI into the NCEP Global Data Assimilation System, Weather Forecast., 24, 1691–1705, 2009.
Lamarque, J.-F. and Hess, P. G.: Cross-tropopause mass exchange and potential vorticity budget in a simulated tropopause folding, J. Atmos. Sci., 51, 2246–2269, 1994.
Langford, A. O., Brioude, J., Cooper, O. R., Senff, C. J., Alvarez II, R. J., Hardesty, R. M., Johnson, B. J., and Oltmans, S. J.: Stratospheric influence on surface ozone in the Los Angeles area during late spring and early summer of 2010, J. Geophys. Res., 117, D00V06, doi:10.1029/2011JD016766, 2012.
Langford, A. O., Aikin, K. C., Eubank, C. S., and Williams, E. J.: Stratospheric contribution to high surface ozone in Colorado during springtime, Geophys. Res. Lett., 36, L12801, doi:10.1029/2009GL038367, 2009.
Lefohn, A. S., Wernli, H., Shadwick, D., Limbach, S., Oltmans, S. J., and Shapiro, M.: The importance of stratospheric-tropospheric transport in affecting surface O_3 mixing ratios in the western United States, Atmos. Environ., 45, 4845–4857, doi:10.1016/j.atmosenv.2011.06.014, 2011.
Lefohn, A. S., Wernli, H., Shadwick, D., Oltmans, S., and Shapiro, M.: Quantifying the importance of stratosphere-troposphere transport on surface ozone concentrations at high-

and low- elevation monitoring sites in the United States, Atmos. Environ., 62, 646–656, doi:10.1016/j.atmosenv.2012.09.004, 2012.
Levelt, P. F., van den Oord, G. H. J., Dobber, M. R., Mälkki, A., Visser, H., de Vries, J., Stammes, P., Lundell, J. O. V., and Saari., H.: The Ozone Monitoring Instrument, IEEE T. Geosci. Remote, 44, 1093–1101, doi:10.1109/TGRS.2006.872333, 2006.
Lin, M., Fiore, A. M., Cooper, O. R., Horowitz, L. W., Langford, A. O., Levy II, H., Johnson, B. J., Naik, V., Oltmans, S. J., and Senff, C. J.: Springtime high surface ozone events over the western United States: quantifying the role of stratospheric intrusions, J. Geophys. Res., 117, D00V22, doi:10.1029/2012JD018151, 2012.
Nakazawa, T., Miyashita, K., Aoki, S., and Tanaka, M.: Temporal and spatial variations of upper troposphere and lower stratospheric carbon dioxide, Tellus B, 43, 106–117, doi:10.1034/j.1600-0889.1991.t01-1-00005.x, 1991.
Pierce, R. B., Schaack, T. K., Al-Saadi, J., Fairlie, T. D., Kittaka, C., Lingenfelser, G., Natarajan, M., Olson, J., Soja, A., Zapotocny, T. H., Lenzen, A., Stobie, J., Johnson, D. R., Avery, M., Sachse, G., Thompson, A., Cohen, R., Dibb, J., Crawford, J., Rault, D., Martin, R., Szykman, J., and Fishman, J.: Chemical data assimilation estimates of continental US ozone and nitrogen budgets during the Intercontinental Chemical Transport Experiment – North America, J. Geophys. Res., 112, D12S21, doi:10.1029/2006JD007722, 2007.
Pierce, R. B., Al-Saadi, J., Kittaka, C., Schaack, T., Lenzen, A., Bowman, K., Szykman, J., Soja, A., Ryerson, T., Thompson, A. M., Bhartia, P., and Morris, G. A.: Impacts of background ozone production on Houston and Dallas, TX Air Quality during the TexAQS field mission, J. Geophys. Res., 114, D00F09, doi:10.1029/2008JD011337, 2009.
Sawa, Y., Machida, T., and Matsueda, H.: Seasonal variations of CO_2 near the tropopause observed by commercial aircraft, J. Geophys. Res., 113, D23301, doi:10.1029/2008JD010568, 2008.
Schaack, T. K., Zapotocny, T. H., Lenzen, A. J., and Johnson, D. R.: Global climate simulation with the University of Wisconsin global hybrid isentropic coordinate model, J. Climate, 17, 2998–2016, 2004.
Søensen, J. H. and Nielson, N. W.: Intrusion of stratospheric ozone to the free troposphere through tropopause folds – a case study, Phys. Chem. Earth Pt. B, 26, 801–806, 2001.
Sprenger, M. and Wernli, H.: A northern hemispheric climatology of cross-tropopause exchange for the ERA15 time period (1979–1993), J. Geophys. Res., 108, 8521, doi:10.1029/2002JD002636, 2003.

ACPD
13, 10157–10192, 2013

Springtime stratosphere-to-troposphere transport

E. L. Yates

Stohl, A., Spichtinger-Rakowsky, N., Bonasoni., P., Feldman, H., Memmesheimer, M., Scheel, H. E., Trickl, T., Hübener, S., Ringer, W., and Mandl, M.: The influence of stratospheric intrusions on alpine ozone concentrations, Atmos. Environ., 34, 1323–1354, 2000.
Stull, R. B.: Meteorology for Scientists and Engineers, 2nd edn., Brooks Cole Publishing Company, Pacific Grove, CA, 502 pp., 2000.
Tadić, J. M., Loewenstein, M., Frankenberg, C., Iraci, L. T., Yates, E. L., Gore, W., and Kuze, A.: A comparison of the aircraft measurements of carbon dioxide to GOSAT data measured over Railroad Valley playa, Nevada, USA, manuscript in preparation, 2013.
Thompson, A. M., Stone, J. B., Witte, J. C., Miller, S. K., Pierce, R. B., Chatfield, R. B., Oltmans, S. J., Cooper, O. R., Loucks, A. L., Taubman, B. F., Johnson, B. J., Joseph, E., Kucsera, T. L., Merrill, J. T., Morris, G. A., Hersey, S., Forbes, G., Newchurch, M. J., Schmidlin, F. J., Tarasick, D. W., Thouret, V., and Cammas, J.-P.: Intercontinental chemical transport experiment Nzonesonde Network Study (IONS) 2004: 1. summertime upper troposphere/lower stratosphere ozone over northeastern North America, J. Geophys. Res., 112, D12S12, doi:10.1029/2006JD007441, 2007.
US Environmental Protection Agency, US EPA: Air quality criteria for ozone and related photochemical oxidants, report EPA/600/R-05/004af, February 2006, US Environmental Protection Agency, Office of Research and Development, Research Triangle Park, NC, 2006.
US Environmental Protection Agency, US EPA: National Ambient Air Quality Standards for Ozone, Federal Register FRL-9102-1, 75 FR 2938, 2938–3052, 2010.
Vaughan, G., Price, J. D., and Howells, A.: Transport into the troposphere in a tropopause fold, Q. J. Roy. Meteor. Soc., 120, 1085–1103, 1994.
Waters, J. W., Froidevaux, L., Harwood, R. S., Jarnot, R. F., Pickett, H. M., Read, W. G., Siegel, P. H., Cofield, R. E., Filipiak, M. J., Flower, D. A., Holden, J. R., Lau, G. K., Livesey, N. J., Manney, G. L., Pumphrey, H. C., Santee, M. L., Wu, D. L., Cuddy, D. T., Lay, R. R., Loo, M. S., Perun, V. S., Schwartz, M. J., Stek, P. C., Thurstans, R. P., Boyles, M. A., Chandra, K. M., Chavez, M. C., Chen, G.-S., Chudasama, B. V., Dodge, R., Fuller, R. A., Girard, M. A., Jiang, J. H., Jiang, Y., Knosp, B. W., LaBelle, R. C., Lam, J. C., Lee, K. A., Miller, D., Oswald, J. E., Patel, N. C., Pukala, D. M., Quintero, O., Scaff, D. M., Snyder, W. V., Tope, M. C., Wagner, P. A., and Walch, M. J.: The Earth Observing System Microwave Limb Sounder (EOS MLS) on the Aura Satellite, IEEE T. Geosci. Remote, 44, 1075–1092,doi:10.1109/TGRS.2006.873771, 2006.

ACPD
13, 10157–10192, 2013

Springtime stratosphere-to-troposphere transport

E. L. Yates

Worden, H. M., Bowman, K. W., Worden, J. R., Eldering, A., and Beer, R.: Satellite measurements of the clear-sky greenhouse effect from tropospheric ozone, Nat. Geosci., 1, 305–308, 2008.

Zanis, P., Trickl, T., Stohl, A., Wernli, H., Cooper, O., Zerefos, C., Gaeggeler, H., Schnabel, C., Tobler, L., Kubik, P. W., Priller, A., Scheel, H. E., Kanter, H. J., Cristofanelli, P., Forster, C., James, P., Gerasopoulos, E., Delcloo, A., Papayannis, A., and Claude, H.: Forecast, observation and modelling of a deep stratospheric intrusion event over Europe, Atmos. Chem. Phys., 3, 763–777, doi:10.5194/acp-3-763-2003, 2003.

Zapotocny, T. H., Lenzen, A. J., Johnson, D. R., Reames, F. M., and Schaack, T. K.: A comparison of inert trace constituent transport between the University of Wisconsin isentropic–sigma model and the NCAR Community Climate Model, Mon. Weather Rev., 125, 120–142, 1997.

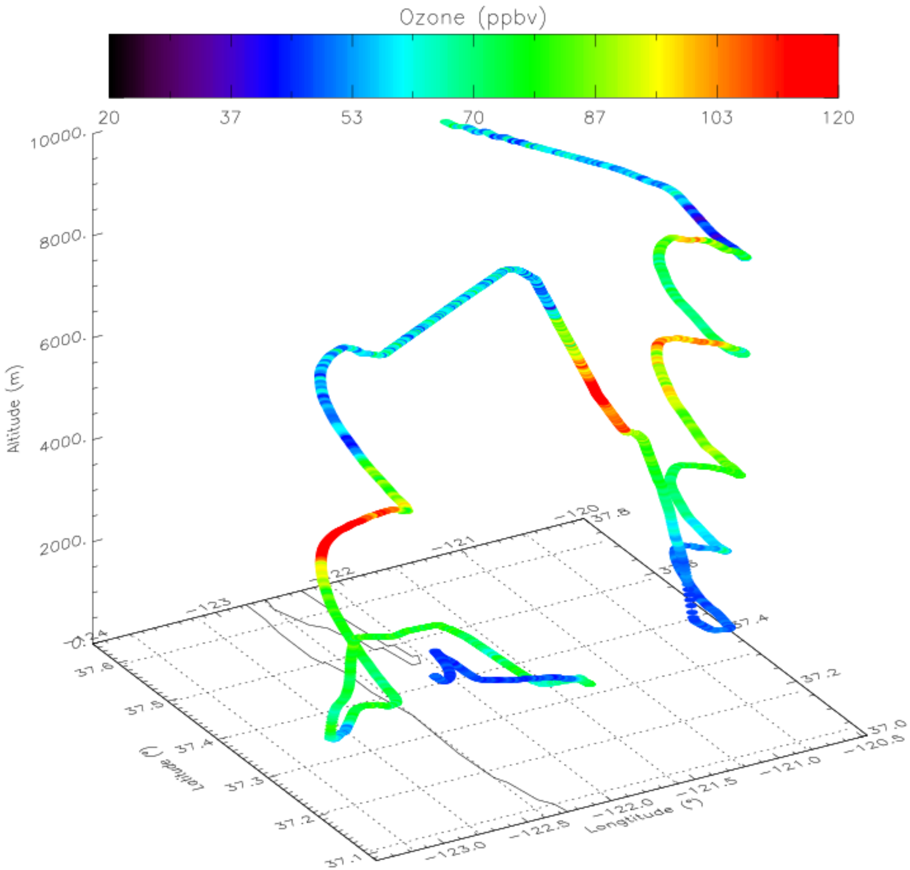

Fig. 1. 3-D projection of O_3 mixing ratio (ppbv) as observed during flight on 14 May 2012 (take-off time: 18:00 UTC). The O_3 monitor requires a 10 min warm-up period before stable measurements are made, which results in data acquisition starting at 8.4 km during the transit to the San Joaquin Valley (inland) site.

ACPD
13, 10157–10192, 2013

Springtime stratosphere-to-troposphere transport

E. L. Yates

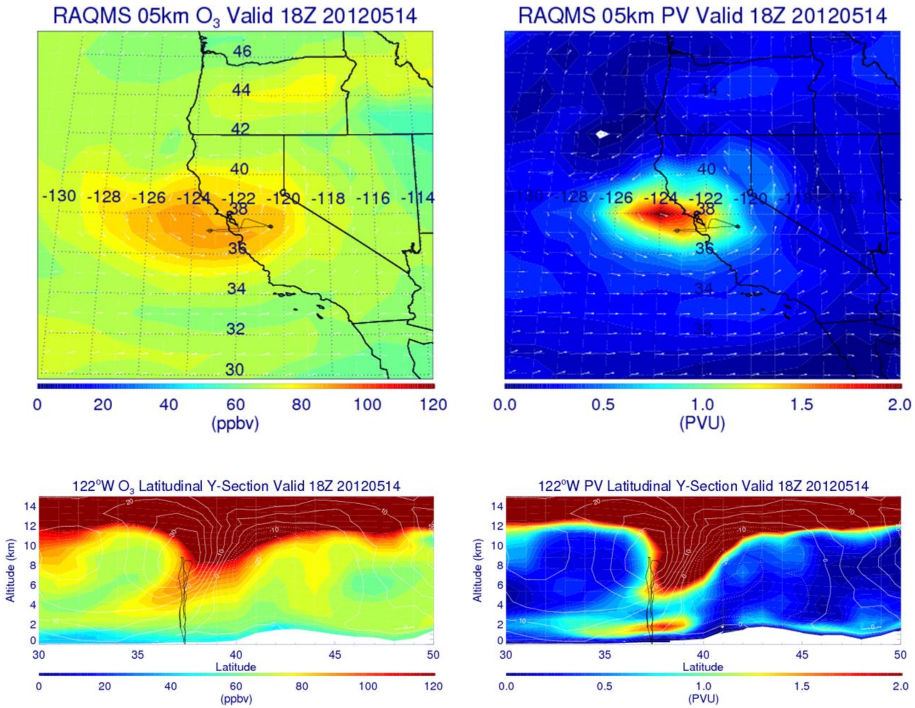

Fig. 2. 5 km O_3 (ppbv) and wind vectors (white, upper left) and PV (PVU) and wind vectors (white, upper right) maps with O_3 (ppbv, lower left) and PV (PVU, lower right) cross sections at 122° W on 14 May 2012 at 18:00 UTC from the RAQMS analyses. The aircraft flight track is shown in black. Note the cut-off low associated with relatively strong PV and high O_3 extending from the lower stratosphere into the mid-troposphere.

ACPD
13, 10157–10192, 2013

Springtime stratosphere-to-troposphere transport

E. L. Yates

ACPD
13, 10157–10192, 2013

Springtime stratosphere-to-troposphere transport

E. L. Yates

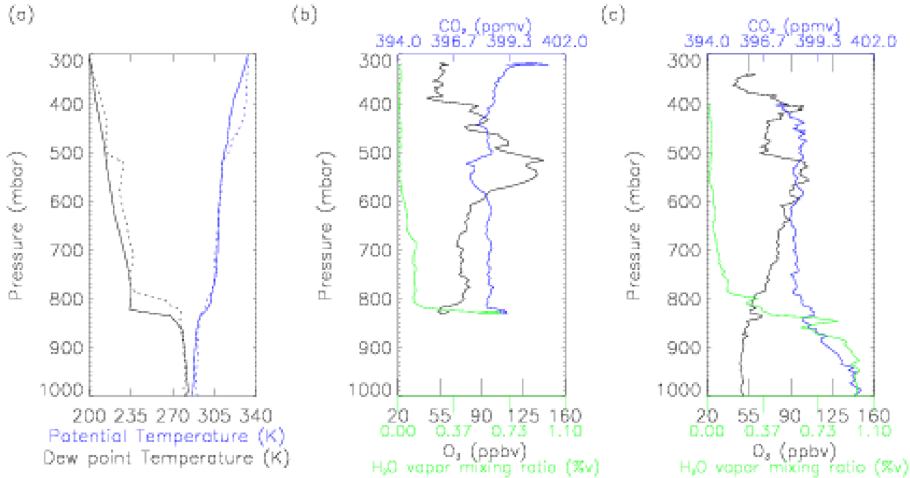

Fig. 3. (a) Potential temperature and dew point soundings at Oakland, CA on 14 May 2012 at 12:00 UTC (dotted lines) and 15 May 2012 at 00:00 UTC (solid lines). Oakland is ~ 140 km from the San Joaquin Valley (inland) site and ~ 100 km from the offshore site. Mixing ratios of O_3 (black), CO_2 (blue) and H_2O (green) observed **(b)** offshore, and **(c)** over the San Joaquin Valley during descending spiral-profiles on 14 May 2012. Note the change of the ozone horizontal scale between panels.

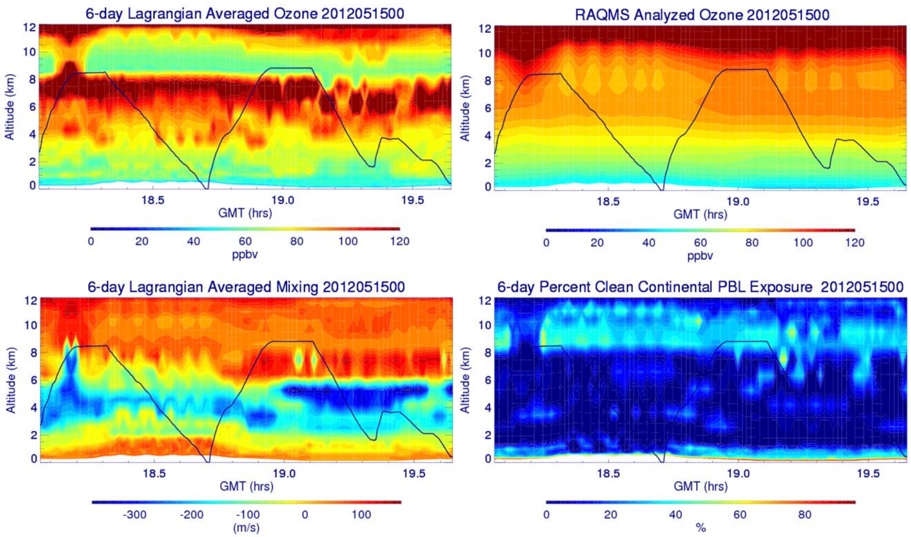

Fig. 4. RAQMS RDF O_3 (ppbv, upper left), Analyzed O_3 (ppbv, upper right), RDF Mixing Efficiency ($m\,s^{-1}$, lower left), and % Clean Continental PBL Exposure (%, lower right) for AJAX flight on 14 May 2012.

ACPD
13, 10157–10192, 2013

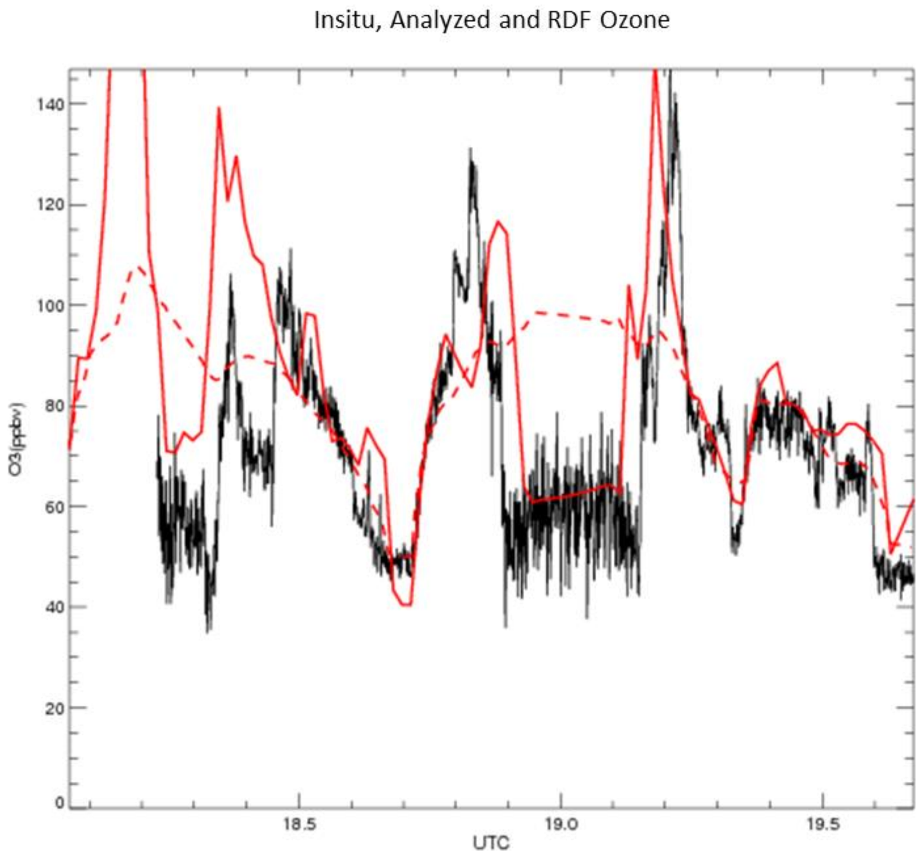

Fig. 5. Timeseries of in-situ (black), RAQMS Reverse Domain Filled (RDF) (solid red), and RAQMS analysed (dashed red) O_3 (ppbv) for AJAX flight on 14 May 2012. The RDF approach provides much better agreement with the in situ observations.

ACPD
13, 10157–10192, 2013

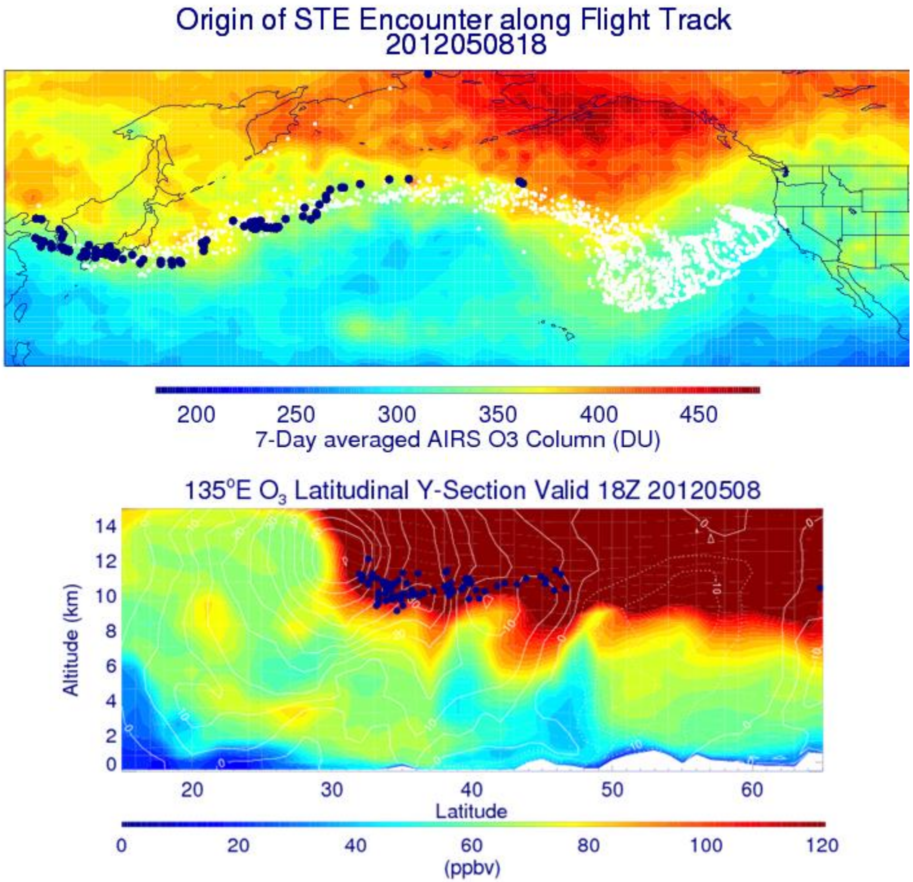

Fig. 6. Map of 7 day averaged (7–14 May 2012) AIRS total column O_3 (DU, top) with the STT back trajectory history (white) and origin (blue). RAQMS 135° E O_3 (ppbv) and zonal wind ($m\,s^{-1}$) cross-section (bottom) with origin of STT encounter (blue dots) at 18:00 UTC on 8 May 2012 for analysis of AJAX flight on 14 May 2012.

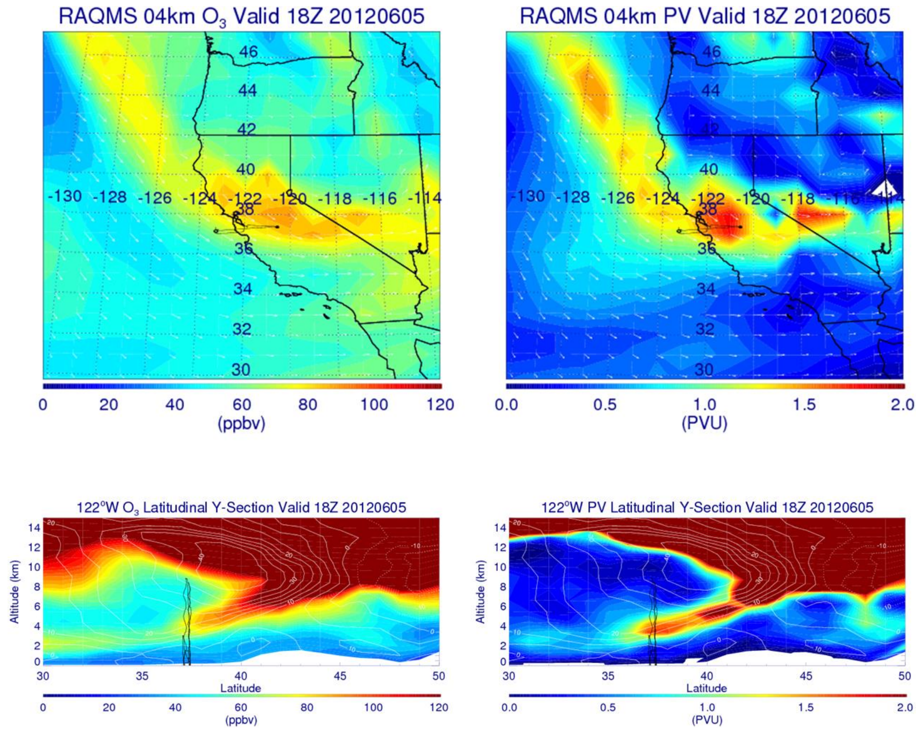

Fig. 7. 4 km O_3 (ppbv) and wind vectors (white, upper left) and PV (PVU) and wind vectors (white, upper right) maps with O_3 (ppbv, lower left) and PV (PVU, lower right) cross sections at 120° W on 5 June 2012 at 18:00 UTC from the RAQMS analyses. The aircraft flight track is shown in black. Note the tropopause fold indicated by the tongue of relatively strong PV and high O_3 extending from the lower stratosphere into the mid-troposphere.

ACPD
13, 10157–10192, 2013

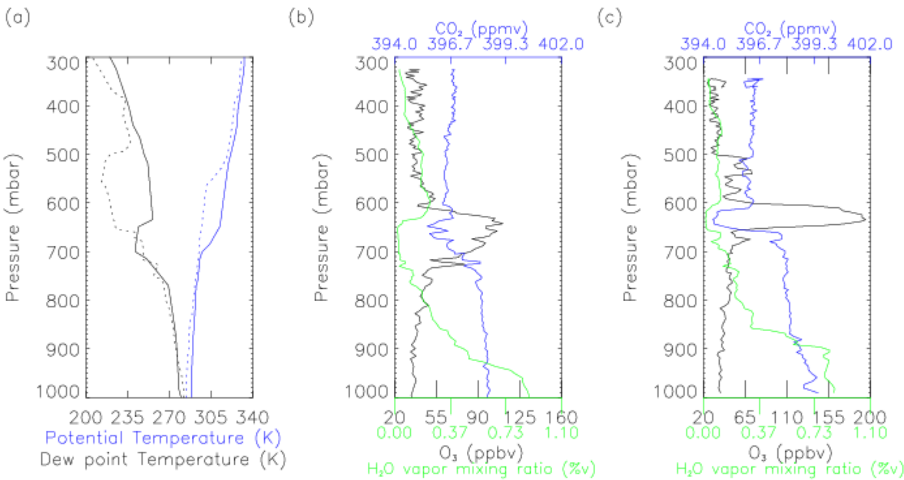

Fig. 8. (a) Potential temperature and dew point soundings at Oakland, CA on 5 June 2012 at 12:00 UTC (dotted lines) and 6 June 2012 at 00:00 UTC (solid lines). Mixing ratios of O_3 (black), CO_2 (blue) and H_2O (green) observed **(b)** offshore, and **(c)** over the San Joaquin Valley during descending spiral-profiles on 5 June 2012. Note the change of the ozone horizontal scale between panels.

ACPD
13, 10157–10192, 2013

Title Page
Abstract Introduction
Conclusions References
Tables Figures
◀I ▶I
◀ ▶
Back Close
Full Screen / Esc
Printer-friendly Version
Interactive Discussion

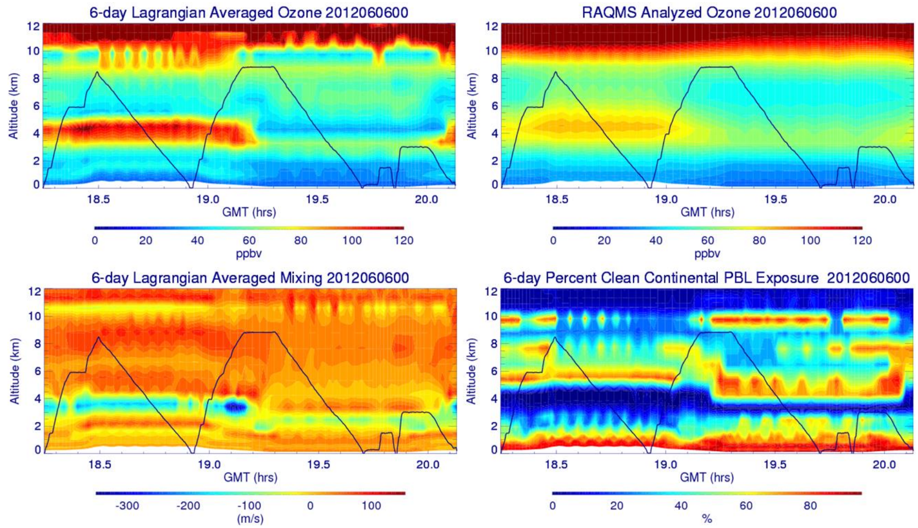

Fig. 9. RAQMS RDF O_3 (ppbv, upper left), Analyzed O_3 (ppbv, upper right), RDF Mixing Efficiency ($m\,s^{-1}$, lower left), and % Clean Continental PBL Exposure (%, lower right) for AJAX flight on 5 June 2012.

ACPD
13, 10157–10192, 2013

Springtime stratosphere-to-troposphere transport

E. L. Yates

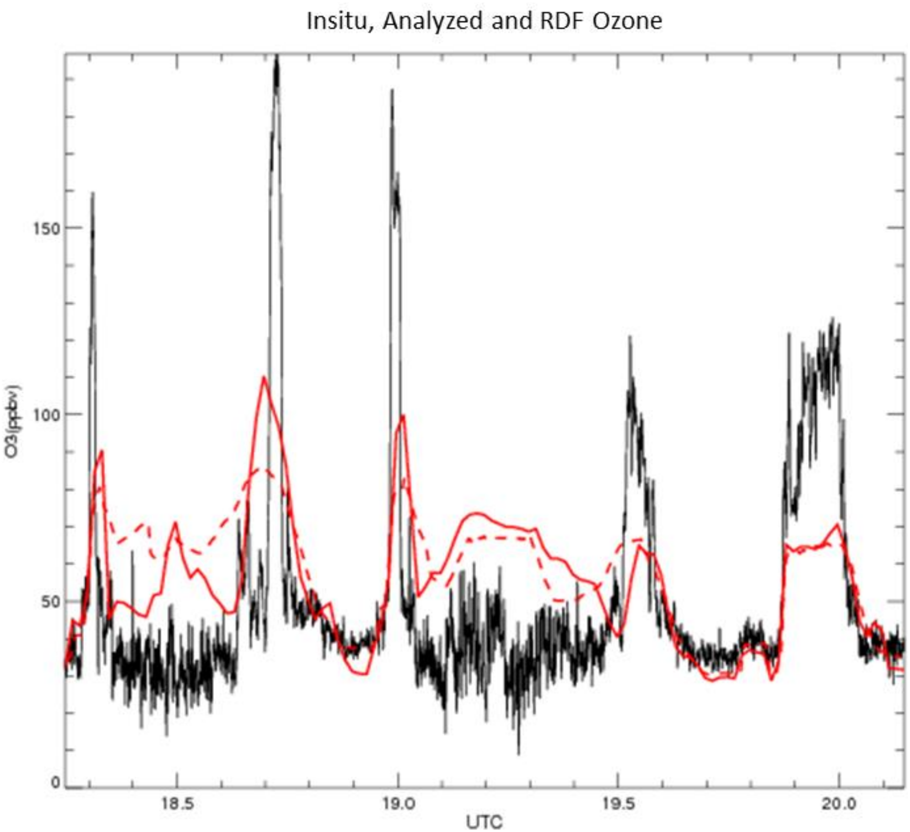

Fig. 10. Timeseries of in-situ (black), RAQMS Reverse Domain Filled (RDF) (solid red), and RAQMS analysed (dashed red) O_3 (ppbv) for AJAX flight on 5 June 2012.

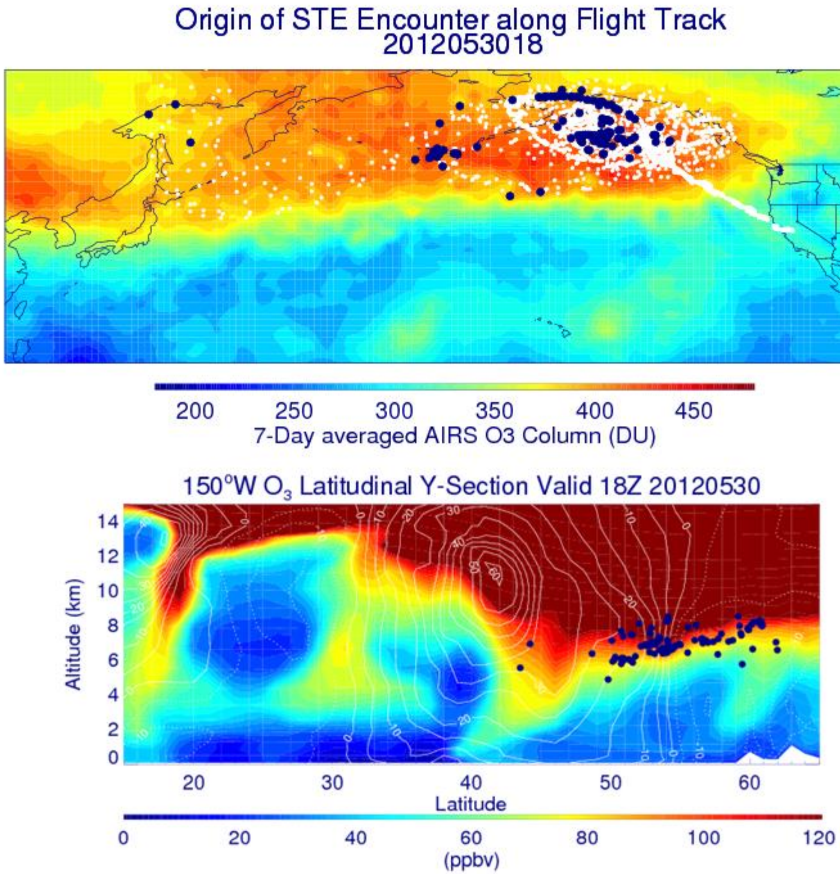

Fig. 11. Map of 7 day averaged (30 May–5 June 2012) AIRS total column O_3 (DU, top) with the STT back trajectory history (white) and origin (blue) and RAQMS 150° W O_3 (ppbv) and zonal wind ($m\,s^{-1}$) cross-section (bottom) with origin of STT encounter (blue dots) at 18:00 UTC on 30 May 2012 for analysis of AJAX flight on 5 June 2012.

ACPD
13, 10157–10192, 2013

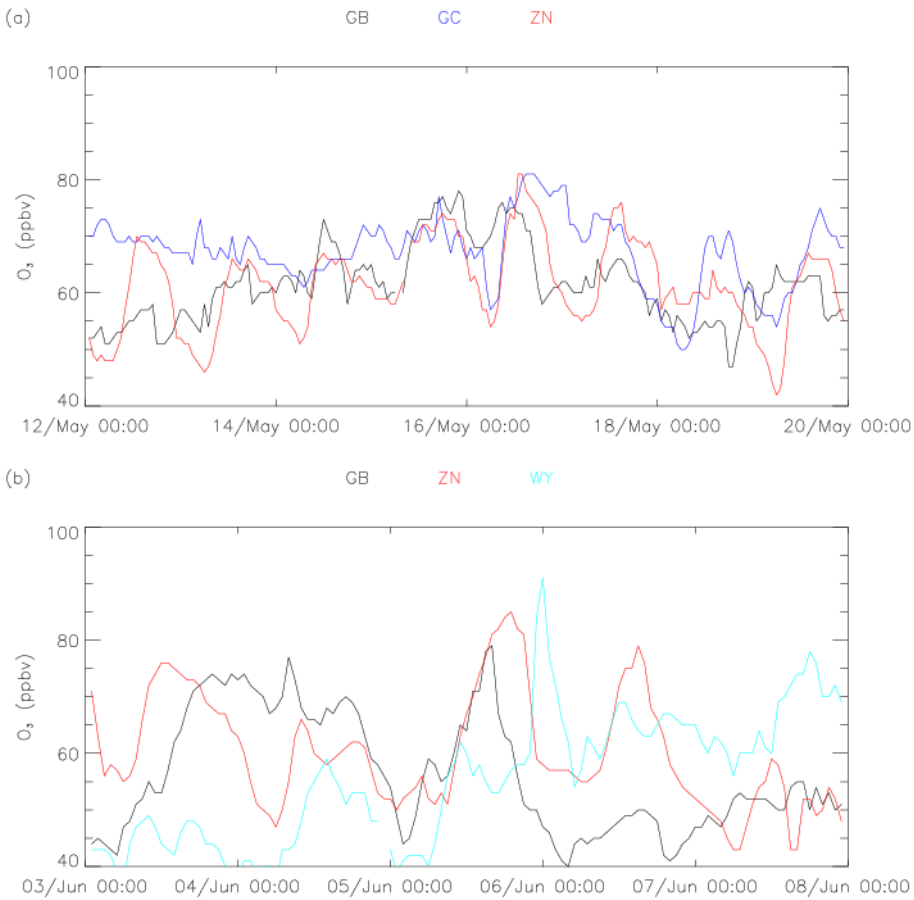

Fig. 12. O_3 Timeseries from surface monitoring sites; Great Basin National Park, Nevada (GB, black), Grand Canyon National Park, Arizona (GC, blue), Zion National Park, Utah (ZN, red), and South Pass, Wyoming (WY, cyan) during 12–19 May 2012 **(a)** and 3–7 June 2012 **(b)**.

ACPD
13, 10157–10192, 2013

Springtime stratosphere-to-troposphere transport

E. L. Yates

Title Page
Abstract Introduction
Conclusions References
Tables Figures
◀| |▶
◀ ▶
Back Close
Full Screen / Esc
Printer-friendly Version
Interactive Discussion